Agricultural and Forest Meteorology 348 (2024) 109912

Contents lists available at ScienceDirect

Agricultural and Forest Meteorology

journal homepage: www.elsevier.com/locate/agrformet

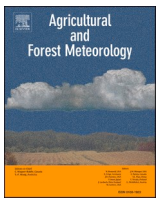

# Structural changes caused by selective logging undermine the thermal buffering capacity of tropical forests

Erone Ghizoni Santos [a,*], Martin Svátek [b], Matheus Henrique Nunes [a,f], Juha Aalto [a,c], Rebecca A. Senior [d], Radim Matula [e], Roman Plichta [b], Eduardo Eiji Maeda [a,c]

[a] Department of Geosciences and Geography, P.O. Box 68, FI-00014 University of Helsinki, Helsinki, Finland
[b] Department of Forest Botany, Dendrology and Geobiocoenology, Mendel University in Brno, Brno, Czech Republic
[c] Finnish Meteorological Institute, P.O. Box 503, FI-00101 Helsinki, Finland
[d] Conservation Ecology Group, Department of Biosciences, Durham University, Durham DH1 3LE, UK
[e] Faculty of Forestry and Wood Sciences, Czech University of Life Sciences Prague, Prague 6 - Suchdol, Czech Republic
[f] Department of Geographical Sciences, University of Maryland, College Park, MD, USA

ARTICLE INFO

*Keywords:*
Microclimate
Temperature
Borneo
TLS
LiDAR
Global warming
Climate change

ABSTRACT

Selective logging is responsible for approximately 50 % of human-induced disturbances in tropical forests. The magnitude of disturbances from logging on the structure of forests varies widely and is associated with a multitude of impacts on the forest microclimate. However, it is still unclear how changes in the spatial arrangement of vegetation arising from selective logging affect the capacity of forests to buffer large-scale climate (i.e., macroclimate) variability. In this study, we leveraged hundreds of terrestrial LiDAR measurements across tropical forests in Malaysian Borneoto quantify the impacts of logging on canopy structural traits, using a space-for-time approach. This information was combined with locally measured microclimate temperatures of the forest understory to evaluate how logging disturbances alter the capacity of tropical forests to buffer macroclimate variability. We found that heavily logged forests were approximately 12 m shorter and had 65 % lower plant area density than unlogged forests, with most plant material allocated in the first 10 m above ground. Heavily logged forests were on average 1.5 °C warmer than unlogged forests. More strikingly, we show that subtle changes in the forest structure were sufficient to reduce the cooling capacity of forests during extremely warm days (e.g., anomalies $> 2\sigma$), while understory temperatures in heavily logged forests were often warmer than the macroclimate under the same conditions. Our results thus demonstrate that selective logging is associated with substantial changes in the fine-scale thermal regime of the understory. Hence, mitigating and managing logging disturbances will be critical for maintaining niches and thermal limits within tropical forests in the future.

## 1. Introduction

The vast majority of environmental changes in tropical forests are induced by human activities (Ellis et al., 2021; FAO, 2011). One of the most extensive of these activities is selective logging, the dynamics of which tend to change over time depending on human needs and socio-economic factors (Nakicenovic et al., 2000). Selective logging is characterized by the harvest of trees of economic interest, and is responsible for 51 % of the forest disturbances in Asia and Latin America (Hosonuma et al., 2012), accounting for approximately 12 % of the total $CO_2$ emissions from forest disturbances in tropical countries (Pearson et al., 2017). The harvesting process also alters the structure and functioning of the forest by reducing tree density, modifying tree species composition, and changing the local climate (Blonder et al., 2018; Milodowski et al., 2021; Pfeifer et al., 2015; Santos et al., 2022). Logging of tall trees reduces the amount of plant material in the upper canopy (Hardwick et al., 2015; Santos et al., 2022) and creates forest gaps (Kumar and Shahabuddin, 2005), which increase light penetration (Fauset et al., 2017) and turbulent air mixing leading to a reduction of evapotranspiration (Good et al., 2015).

As a result of the physical changes that occur in the forest, the fine-scale climatic conditions below the canopy, here defined as the forest

* Corresponding author.
*E-mail address:* erone.ghizonisantos@helsinki.fi (E.G. Santos).

https://doi.org/10.1016/j.agrformet.2024.109912
Received 8 September 2023; Received in revised form 25 January 2024; Accepted 26 January 2024
Available online 12 February 2024

microclimate, are also impacted. The microclimate is regulated by a combination of the macroclimate (De Frenne et al., 2021), local water availability (Davis et al., 2019), soil, topography, and vegetation structure (Geiger et al., 2009). It is, therefore, directly linked to activities that affect the forest structure (Hardwick et al., 2015; Jucker et al., 2018). The variability in the vertical profile of the forest canopy could modulate the relationship between microclimate and macroclimate, thus controlling attributes such as temperature offset and temperature range, hereafter referred as thermal metrics. The first metric is defined as the difference in temperature between the macroclimate and the microclimate, with negative values representing a relatively warmer microclimate and positive values representing a cooler microclimate (De Frenne et al., 2021). While the second metric (temperature range) represents the difference between maximum and minimum temperatures (De Frenne et al., 2021).

Forest microclimates greatly influence forest functioning, including soil respiration, nutrient cycling, and plant regeneration (Chen et al., 1999; Smith and Johnson, 2004), and can affect forest ecosystem responses to climate change (Stevens et al., 2015). Ecosystem dynamics can be more closely linked to variations in microclimate rather than in macroclimate (De Frenne et al., 2021) with amplified microclimate temperature fluctuation in open areas (Gril et al., 2022). Nevertheless, uncertainties persist in understanding the thermal characteristics of microclimates affected by logging due to limitations in acquiring microclimate data and the lack of quantitative methods to assess structural changes in tropical forests. While selective logging is known to induce structural changes resulting in elevated microclimate temperatures in tropical forests (Blonder et al., 2018), recent studies suggest that impacts of selective logging can be short-lived (Senior et al., 2017a).

Recently, increased access to Light Detection and Ranging (LiDAR) technologies has enabled a more precise monitoring of forest structural attributes and a more robust understanding of the relationships between biophysical parameters and microclimate. In particular, Terrestrial Laser Scanning (TLS) systems can quantify the three-dimensional distribution of plant material in high detail, even in dense tropical forests where aerial and spaceborne platforms have difficulties in characterizing the understory vegetation (Calders et al., 2020; Maeda et al., 2022; Santos et al., 2022). A potentially effective method for analysing the intricate data obtained from TLS systems involves calculating canopy structural metrics, commonly known as canopy structural traits (Schneider et al., 2019). These traits encompass physical attributes that offer insights into the vertical arrangement of the forest, encompassing details about the diversity and distribution of materials within the vertical profile. In combination with improved instrumentation capability for monitoring microclimate (Wild et al., 2019), these recent advances can offer new insights into the microclimatic conditions of logged forests and how forests will respond to increasing climatic variability.

The objective of this study was to investigate how structural changes arising from selective logging affect the forest capacity to buffer temperature variability. The following research questions were addressed: 1. How do changes in forest structural traits caused by logging affect microclimate patterns on a diurnal and seasonal basis? 2. Are observed changes in forest structure associated with predicted changes in the daily and seasonal patterns of microclimate temperature? To answer these questions, we used forest structure data derived from over 280 TLS measurements combined with in-situ microclimate measurements and high temporal resolution macroclimate data.

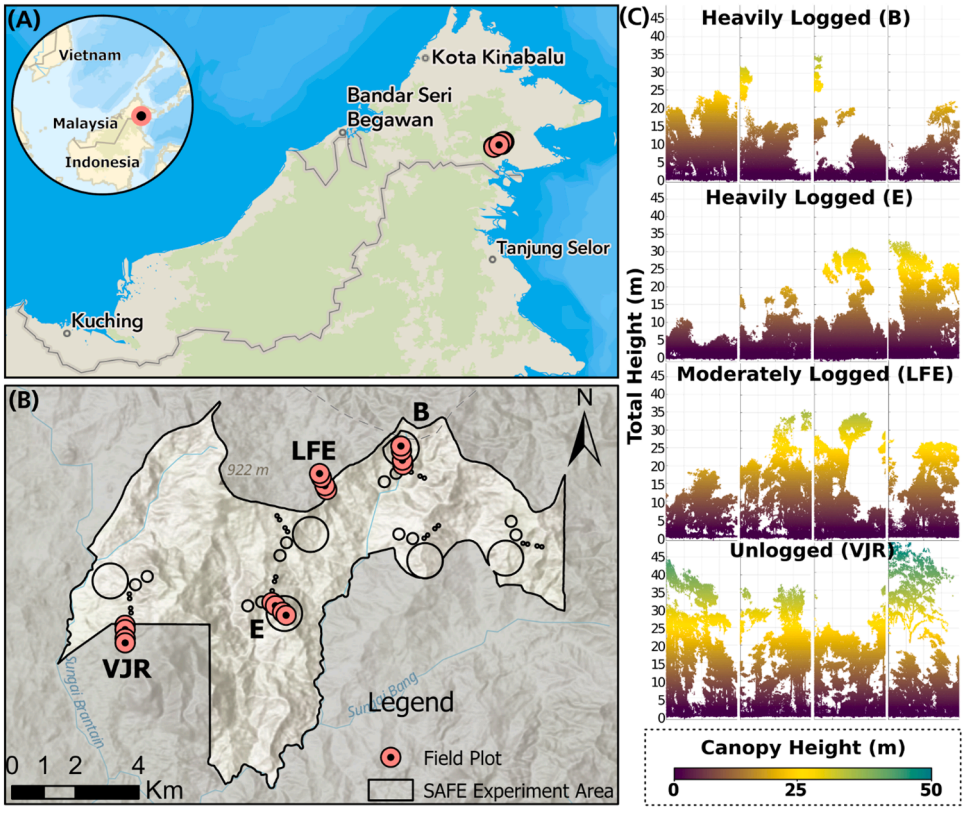


**Fig. 1.** Location of the study area and the plots within the SAFE experiment, where the TLS and the microclimate data were collected. Panel (A) depicts the geographic location of Malaysia on the island of Borneoand the plot location. The SAFE project area and the location of the field plots are shown in (B). Panel (C) depicts a slice (5 m x 20 m) in the middle of each plot for the vertical profile as detected by TLS. In total, there were four blocks with four plots each distributed across three classes of logging: heavily logged (B and E), moderately logged (LFE) and unlogged (VJR).

## 2. Materials and methods

### 2.1. Study area

The study area is located between 4°41′12″N and 4°44′20″N, 117°30′50″E and 117°38′56″E in the Malaysian state of Sabah, on the island of Borneo(Fig. 1). The climate is characterized as humid tropical, with annual accumulated precipitation between 2600 mm and 2700 mm, and an average annual temperature around 27 °C (Walsh and Newbery, 1999). The area is considered aseasonal, as it lacks clear dry/rainy seasons. However, precipitation may be substantially reduced during El Niño Southern Oscillation (ENSO) events (Katayama et al., 2009; Nunes et al., 2021).

Our plots were located in the Stability of Altered Forest Ecosystems (SAFE) project region, the world's largest forest fragmentation experiment (Ewers et al., 2011). The SAFE project is in an area gazetted for conversion to oil palm plantations. As oil palm plantations are established, fragments of logged forests are being protected as part of an experiment that investigates the impacts of logging and fragmentation on biodiversity and ecosystem functioning (Ewers et al., 2011).

The SAFE project area connects 2200 ha of intact areas to forests that underwent selective logging several times in the past. Only approximately 8 % of the area remains unlogged, and most of that is located in protected areas. In addition, it is estimated that 80 % of the forests were affected by logging in the 1990s and 2000s (Bryan et al., 2013). Thus, human activities resulted in areas with highly heterogeneous structure (Pfeifer et al., 2016; Reynolds et al., 2011) and high presence of pioneer species, which increase in abundance with increasing intensity of disturbance (Riutta et al., 2018).

Our data were collected from sixteen 25 m x 25 m plots equally distributed over different SAFE project blocks B, E, LFE (Continuous Logged Forest) and in a protected adjacent area, VJR (Virgin Jungle Reserve) (Fig. 1B). The SAFE area was logged in the past one to four times, targeting commercially valuable species in the genera *Dipterocarpus, Dryobalanops, Shorea* and *Parashorea*. The first logging round took place around the 1970s, targeting trees with stems $>$ 0.6 m diameter at breast height, resulting in approximately 113 $m^3$ $ha^{-1}$ of timber harvested (Fisher et al., 2011). Between 2001 and 2007, the area underwent the second logging cycle with a diameter at breast height target of $>$ 0.4 m. On average, around 31 $m^3$ $ha^{-1}$ of wood were harvested from SAFE area (Fisher et al., 2011). However, during the second rotation, blocks B and E were harvested three times, which led to an accumulated 66 $m^3$ $ha^{-1}$ of wood extraction (Struebig et al., 2013). In the LFE block, 37 $m^3$ $ha^{-1}$ of wood was harvested in the second rotation (Struebig et al., 2013). VJR is an area adjacent to the SAFE experiment, which was minimally logged in the past only on the borders of the fragment for the construction of access roads, with the interior remaining undisturbed with basal area similar to one of the best preserved old-growth forests in Borneo, Danum Valley Conservation Area. Said that, we considered VJR as unlogged/intact forest.

Due to variation in the amount of wood harvested in each block, the SAFE project area represents a logging disturbance gradient, herein described by classes of logging to differentiate the areas impacted by logging in terms of amount of wood harvested. The classes range from heavily logged forests (B and E blocks) followed by moderately logged forests (LFE block) to unlogged forests (VJR).

### 2.2. Microclimate data

Microclimate data for the entire year of 2019 were collected in the four blocks, B, E, LFE and VJR by placing a TOMST TMS-4 datalogger (TOMST, Prague, Czech Republic) (Wild et al., 2019) in the center of each plot (see Fig. S1 for more details). This datalogger collected temperatures at three different heights, soil (−6 cm), surface (+2 cm) and air (+15 cm) temperatures, recorded every 15 min. TMS-4 dataloggers measure temperatures between −60 °C and +85 °C with a resolution of 0.0625 °C and an accuracy of ±0.5 °C. Here, we focused only on air temperature. The temperature in the sensor is sensible to direct radiation (Maclean et al., 2021), to avoid potential impacts of that effect, we filtered the temperature by removing all values over the 98th percentile. This remotion was made for each datalogger in the raw measurements, which were taken every 15 min. We evaluated the influence of filtering the data by conducting a sensitivity analysis by comparing the results filtering and not filtering the data.

### 2.3. Macroclimate data

The macroclimate temperature was derived from ERA5-Land atmospheric reanalysis by the European Centre for Medium-Range Weather Forecasts, which is a downscaled re-simulation of the land component of global ERA5 reanalysis (Hersbach et al., 2020; Muñoz Sabater, 2019). The dataset has a spatial resolution of ~9 km and it extends hourly data from 1950 to present.

ERA5-Land data is produced using a reanalysis technique, where a diverse set of observational data, including satellite observations and ground-based measurements, are incorporated into a numerical weather model. This process aims to establish a coherent, gridded depiction of Earth's climate. For this study, we used 2 m air temperature estimates from ERA5-Land as a measure of macroclimate temperature, obtained from the platform Climate Data Store for the period of 1989–2019 (30 years). The 2 m temperature data in ERA5-Land represents the air temperature at a height of 2 m above the Earth's surface. As a modeled data, ERA5-Land presents some uncertainties such as observational data quality, model representation, and data assimilation techniques. ERA5-Land demonstrates the capability to accurately capture temperature trends, and variability (Yilmaz, 2023; Zhao et al., 2023). Moreover, ERA5-Land is sensitive to daily and monthly changes, including fluctuations in temperature throughout the day, when compared to weather stations (Zou et al., 2022).

In this study, we assumed that the 2 m macroclimate air temperature data provided a consistent view of the atmospheric conditions above the forest canopy. The spatial sampling of the plots within the SAFE project was designed to minimize confounding factors associated with topography, i.e., the maximum altitude difference between plots was 70 m. Hence, we assume that temperature differences due to vertical lapse rate effects were not substantial and did not confound the analysis undertaken in this study.

### 2.4. Thermal metrics

We calculated the thermal metrics for two different temporal scales for the year 2019, diurnal where the temperatures were aggregated by hour, and daily where the temperatures were aggregated by day for both microclimate and macroclimate. From macroclimate and microclimate in both temporal scales we estimated the minimum, mean and maximum temperatures, $T_{Macro_{Min}}$, $T_{Macro_{Mean}}$, $T_{Macro_{Max}}$, $T_{Micro_{Min}}$, $T_{Micro_{Mean}}$, and $T_{Micro_{Max}}$ respectively.

In addition, from macroclimate data we calculated the average temperature of the period from 1989 to 2018 ($\overline{T}_{Macro_{1989-2018_i}}$) and standard deviation ($\sigma_{\overline{T}_{Macro_{1989-2018_i}}}$) for each day of the year to reflect normal climatological conditions. For this analysis we removed the years with Oceanic Niño Index (NOAA, 2019a,b) greater than or equal to 1 °C to prevent these abnormal years from influencing the calculation of macroclimatic anomalies. The years removed were 1997, 1998, 2014, 2015, and 2016. Finally, we estimated the daily macroclimate anomaly normalized by standard deviation for each day of 2019, which represents how many standard deviations the daily average temperature differs from the historical average (Table 1, Eq. 1).

To compare the macroclimatic and microclimatic temperatures, we computed minimum, mean and maximum temperature offsets, using Eq. 2, 3 and 4, respectively. The offset is the difference between macro-

**Table 1**
Thermal metrics used in this study and their respective equations.

| Trait | Equation | |
|---|---|---|
| Anomaly | $Anomaly_i = \frac{T_{Macro_{2019_i}} - \overline{T}_{Macro_{1989-2018_i}}}{\sigma_{T_{Macro_{1989-2018_i}}}}$ | (1) |
| Offset Minimum | $Offset_{Min_i} = T_{Macro_{Min_i}} - T_{Micro_{Min_i}}$ | (2) |
| Offset Mean | $Offset_{Mean_i} = T_{Macro_{Mean_i}} - T_{Micro_{Mean_i}}$ | (3) |
| Offset Maximum | $Offset_{Max_i} = T_{Macro_{Max_i}} - T_{Micro_{Max_i}}$ | (4) |
| Diurnal range | $Range_i = T_{Micro_{Max_i}} - T_{Micro_{Min_i}}$ | (5) |
| | where $i$ represents the day of the year. | |
| | $\overline{T}$ is the average of the $i$-th day | |

climate and microclimate temperatures (De Frenne et al., 2021). Additionally, we computed the microclimatic diurnal range (*Range*, Eq.5), which is the difference between the maximum and minimum temperature in the forest microclimate in a 24 h period. These metrics were calculated for all days of the year 2019.

### 2.5. Terrestrial LiDAR data

Terrestrial Laser Scanner data collection took place in November 2019 using a RIEGL VZ-400i laser scanner. We used a vertical and horizontal resolution of 40 mdeg. The frequency used was 0.6 MHz, with a beam divergence of 0.35 mrad allowing for a measurement range of up to 350 m, recording up to eight returns per pulse, which resulted in a point spacing of 0.034 m at 50 m distance from the scanner. The scanner emitted pulses with a wavelength of 1550 nm, with a field of view of 360° in the horizontal axis, and 100° in the vertical axis.

We followed the methodology used by Wilkes et al. (2017) for the TLS acquisition, and the plots consisted of three by three grids, with measurements taken every 10 m, resulting in nine scan positions in each plot (see Fig. S.1 for a plot design scheme). As the scanner has a 100° field of view in the vertical plane, a second scan was performed in each location, with the scanner in the horizontal position by tilting the instrument 90°, resulting in the sampling of the full hemisphere in each scan location. As a result, each scan location was scanned twice, once with the scanner in the horizontal and once with the scanner in the vertical position, totalling more than 280 measurements over the 16 plots.

The individual scans were co-registered using the RIEGL RiSCAN PRO® v2.9 software. This process consisted of adjusting each scan location, moving the point cloud in three rotations (pitch, yaw, roll) and in three axes (x, y, z). We kept the adjustment error below 5 mm and carefully proceeded with visual inspections to ensure that the registration process was successful. Lastly, Digital Terrain Models (DTM) were constructed using LAStools software (Isenburg, 2016) for each plot.

We used a voxel approach to derive vertical canopy structural traits on the software AMAPVox version 1.6.1 (Vincent et al., 2017). AMAPVox tracks each laser pulse through a defined 3D grid to the last return, and then computes the local attenuation in each voxel from the optical path length of each pulse inside of the voxel and the sampling area of each laser pulse. The sampling area of each laser pulse was computed by the combination of the theoretical pulse beam section and the residual beam fraction in a voxel space. Following the assumption that the angles in the vegetation components are spherically distributed (Béland et al., 2011), we estimated the Plant Area Density (PAD, $m^2\ m^{-3}$) by dividing the attenuation by 0.5. Additionally, we estimated other canopy structural traits, such as Plant Area Index (PAI), and layered PAI in every 5 m of the vertical profile, Relative Height (RH), Canopy Ratio (CR), Foliage Height Diversity (FHD), and Effective Number of Layers (ENL).

The PAI was defined as the projected area of the vegetation per unit of ground surface area (Vincent et al., 2017), and it was estimated by the sum of PAD values in each column (PAI = ΣPAD) (Schneider et al., 2017, 2014). Hence, PAI ($m^2\ m^{-2}$) provides an integrated measure of the number of leaves and wood allocated over the vertical column. The RH describes the distribution of material from the ground at a specific height (Drake et al., 2002). For instance, RH75 of 15 m means that 75 % of all material is distributed below 15 m of the height from the ground. We calculated the RHs at two percentiles, 25 % and 98 %, which were used to compute the CR. This trait reflects the ratio between the canopy's depth (RH98 minus RH25) and the total height (RH98). The CR values below 0.74 indicate a forest stand where the material is mostly concentrated in the upper stratum, while values above 0.74 indicate that the plant material is concentrated in the lower layers of the canopy (Schneider et al., 2020). The FHD (MacArthur and MacArthur, 1961) was calculated by applying the Shannon-Wiener diversity index on vertical profiles of PAD. It expresses the number of layers in the vertical profile of the forest and the evenness of the plant surface distribution among vertical canopy layers. The higher the FHD, the greater the number of canopy layers. Higher values also indicate greater habitat complexity (Schneider et al., 2017). Lastly, we estimated the ENL, which is a measure that describes vertical structure taking into account the vertical layers and their respective occupation by tree structures relative to the total space occupation (Ehbrecht et al., 2016). Higher values of ENL indicate more vegetation layers, or a multi-layered stand.

### 2.6. Statistical analyses

We combined TLS-derived structural traits, microclimate, and macroclimate temperatures to analyse how temperature varies across two different temporal scales, diurnal, and seasonal under heavily, moderately, and not logged forest conditions. First, we analysed the Pearson correlation among the structural traits and their distribution across the logging classes and microclimate and macroclimate temperature patterns in a period of 24 h. This was processed with an exploratory analysis for both structural traits and thermal metrics (Section 3.1 and 3.2).

The seasonal temporal scale (Section 3.3) represents the temperature patterns for the year 2019. We aggregated the temperature by day, ending with 365 values for minimum, mean and maximum daily temperatures. Similar to Section 3.2, we proceeded with an exploratory analysis evaluating the influence of logging on the seasonal variability of minimum, mean and maximum temperatures. In addition, we estimated the macroclimate anomalies derived from ERA5-Land as a baseline to investigate the thermal metrics patterns in relation to structural traits (Section 3.4). Mixed models were trained to explain the relationship between offset temperatures and macroclimate temperature with the influence of forest structure. These models had as response variable the offset for temperature minimum, mean, maximum and temperature range. Plot identity was used as a random factor (slope and intercept) to consider the variation within the plots that are not related to changes in forest structure. Forest structural traits and macroclimate anomaly were defined as fixed effects.

We combined structural traits two by two to fit explanatory models. Highly correlated traits were not included in the same model to avoid inflation of model explanatory power due to multicollinearity. The ecological relevance of each trait was also considered to be included in the models (Santos et al., 2022). We assumed that canopy structure remained unaffected during the year 2019, as the plant area index during non-El Niño years can be similar in these forest plots throughout the year (Nunes et al., 2021), thereby having potentially small influences on the structural traits of our analysis. To demonstrate that no substantial variability is expected in the forest structure in SAFE area, we demonstrated the NDVI time-series over the SAFE region plots (see Fig. S2), which show constant values throughout the series, except when the region started to be converted from forest to palm oil plantations, around 2015.

In order to evaluate our analyses, we performed two sensitivity analyses (see Supplementary Material). Firstly, we compared the result by filtering and not filtering the microclimate data at 98th percentile, to evaluate the influence of anomalous values due to heatshield effect. Also, another sensitivity analysis was conducted to investigate if

individuals plots would affect the estimates in our analysis. To validate all the models, we performed 1000 bootstrap iterations, by randomly resampling the data in training and test datasets. We evaluated the uncertainty associated to each model by estimating the distribution through the bootstrap by recording the conditional $R^2$ for the overall model and for each predictor (partitioned $R^2$) in each bootstrap interaction. All the analyses were conducted in R (R Core Team, 2020), to run the mixed models we used the *lme4* package (Bates et al., 2015) and for the partitioned $R^2$ the package *partR2* (Stoffel et al., 2020). Additionally, no specific function or package was developed here to process the data.

Since TLS measurements and microclimate data were not available before the logging (1970s, - 2001–2007), our analyses are based on a space-for-time approach. The method presupposes that geographically distinct sites chosen according to ecological or environmental gradients can function as substitutes for forecasting ecological time series, such as vegetation succession (Fukami and Wardle, 2005; Pickett, 1989; Pickett and White, 1985). This assumption is valid in SAFE, because the project was designed to minimize the effects of confounding factors, such as elevation and slope.

## 3. Results

### 3.1. Vertical forest structure

The correlation of structural traits varied in terms of each other (Fig. S3). The CR presented the lowest correlation among other traits followed by PAI(30–35). Most of the differences between logging classes were evident in the plant material allocation of the middle and upper canopy layers (Fig. 2A), with less plant material (i.e., branches of tall trees) in heavily logged forests. Heavily logged, moderately logged and unlogged forests had average PAIs of 6.7 $m^2$ $m^{-2}$, 9 $m^2$ $m^{-2}$, and 9.8 $m^2$ $m^{-2}$, respectively, and canopy height of 10.5 m, 18.2 m and 27.6 m, respectively.

Within the logging disturbance gradient encompassing heavily logged (composed by blocks B and E), moderately logged (block LFE) and unlogged forests (block VJR), heavily logged forests had a relative higher proportion of plant material allocated in the lower layers (0 to 10 m above ground – see Fig. 2A). Moderately logged forests had more plant material at the medium-upper layer of the canopy while unlogged forests, despite having a similar vertical plant distribution as in moderately logged stands, had a larger amount of plant material in the upper layers above 30 m (refer to Fig. S4).

### 3.2. Diurnal microclimate patterns

Our temperature measurements revealed that heavily logged forests had the highest mean temperatures during the day. However, this pattern was inverted at night-time (18 h to 6 h), with unlogged forests being warmer than heavily logged forests (Fig. 2B). The minimum diurnal temperatures were similar across all three logging classes (Fig. S5A). However, in the early morning (4 h to 8 h) unlogged forests had higher minimum temperatures than heavily logged and moderately logged forests, 0.7 °C and 1.6 °C respectively. On the other hand, for the maximum diurnal temperature (Fig. S5B) between 6 h to 18 h, the heavily logged forests were approximately 1.8 °C warmer than moderately logged and 2.5 °C warmer than unlogged forests on average. Furthermore, during nighttime all three classes of logging presented similar temperatures, unlogged forests tended to be slightly warmer than heavily logged forests by 0.5 °C. However, note sensor accuracy is only 0.5 °C, which limits the precision with which we can detect differences in temperature.

### 3.3. Seasonal microclimate variability

The minimum, maximum and mean daily macroclimate and microclimate temperatures demonstrate seasonal patterns that were inconsistent throughout the year (Fig. 3A–C). A relatively warmer period was observed between April 2019 and July 2019, thus exceeding the temperatures between August and December 2019. The magnitude of the seasonal fluctuations depended on the logging history as well as the thermal trait.

The minimum daily microclimate temperatures were cooler than the minimal macroclimate temperatures throughout the year and across all the logging classes (Fig. 3A). Unlogged forests had lower minimum microclimate daily temperatures than moderately and heavily logged forests. Additionally, unlogged forests did not present high temperature fluctuation across the year (i.e., within-block temperature amplitude was 1.9 °C). In contrast, this fluctuation was more pronounced in moderately and heavily logged forests for the minimum temperature (3 °C).

The seasonal patterns of mean daily temperature across 2019 showed more similarities among the logging classes in terms of temperature

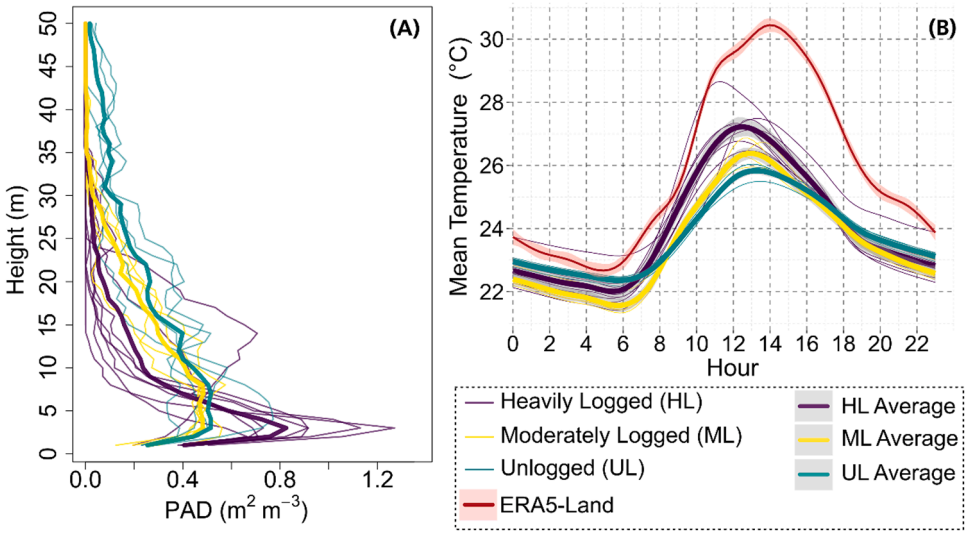


**Fig. 2.** In (A) the distribution of PAD along the vertical profile for all plots with the average values in the thickest lines. In (B), the mean diurnal temperature quantified for each plot in heavily logged (purple), moderately logged (yellow), and unlogged (teal) classes of logging. The thickest lines represent the average among the curves in each class of logging. The red line represents the macroclimate temperature in ERA5-Land data. The grey and red shadows in the means and ERA5-Land curves represent the interval of confidence. For mean and minimum temperatures, see Fig. S.5.

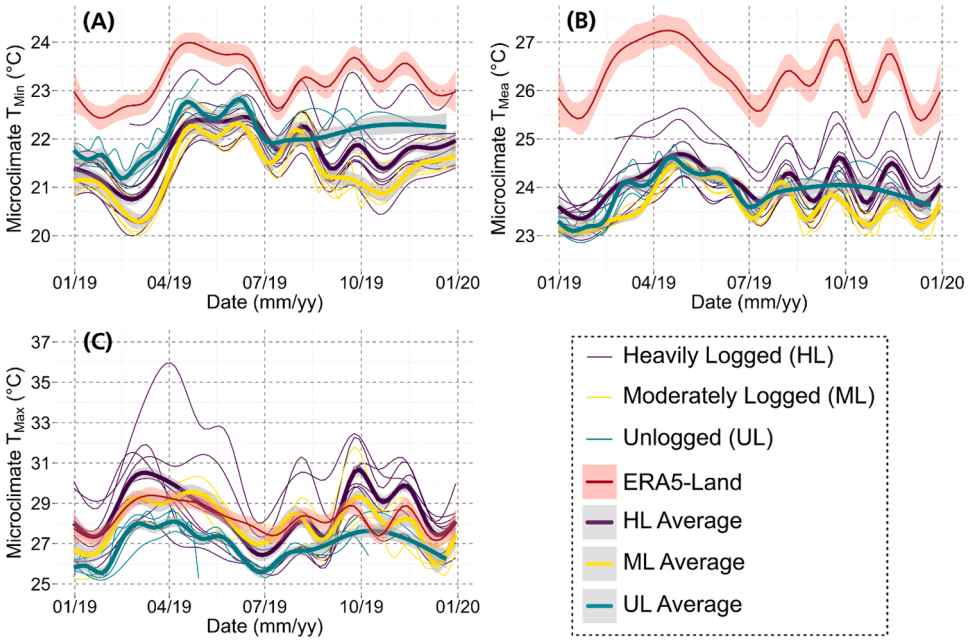


**Fig. 3.** Minimum (A), mean (B) and maximum (C) daily air temperature for heavily logged (purple), moderately logged (yellow) and unlogged (teal) plots. Each curve represents the temperature based on 96 measurements in 24 h for each day in 2019. The red line represents the temperature outside of the forest calculated with ERA5-Land data. The thickest lines represent the average, and the grey shading represents the confidence interval of the curves.

fluctuation over the period, except for two plots in the heavily logged block, which presented warmer mean daily temperatures than the others (See Table S.1 and Fig. S6 for a sensitivity analysis when removing the warmer plot in HL category). The average temperature for the entire period analysed here in the macroclimate was approximately 1.5 °C and 2.5 °C warmer than heavily logged and unlogged, respectively. The amplitude of mean temperature in unlogged forests was lower than in forests affected by logging. Fig. 3B shows how the amplitude of mean temperatures in unlogged forests was less pronounced than in moderately and heavily logged forests.

The maximum daily temperature presented the highest fluctuations of temperature (Fig. 3C). While the maximum macroclimate temperatures were steady, forests affected by logging, and with lower PAI, had a large fluctuation in maximum temperature. The seasonal amplitude of maximum daily temperature decreased in unlogged forests that had typically higher PAI and canopy height. The amplitude, on average, in seasonal maximum daily temperature in unlogged plots was between 25.5 °C and 29 °C (3.5 °C) while in heavily logged plots the amplitude was between 25.2 °C and 36.7 °C (11.5 °C). These findings demonstrate a two-fold variability in mean of maximum temperatures linked to logging intensity.

### 3.4. *Thermal metrics under extreme climatic events*

The intricate relationship between microclimate and macroclimate temperatures, demonstrated that thermal traits behave differently in relation to macroclimate temperature anomalies. It influences temperature dynamics across different logging intensities and its implications for the forest's capacity to buffer climatic variability. Fig. 4 shows how microclimate temperatures are related to macroclimate temperature anomalies. Positive offset values indicate that macroclimate temperatures are higher than microclimate temperatures, while negative values indicate that understory temperatures are lower than macroclimate temperatures. As the macroclimate warms relative to historical average conditions (i.e., anomaly), the minimum temperature offset increased across all classes of logging intensity (Fig. 4A). Unlogged forests had consistently lower minimum temperature offsets than heavily and moderately logged forests, which indicates that logged forests had lower minimum temperatures than unlogged forests, during either cold or hot days. Differences in the mean offset temperatures across the gradient in logging intensity were smaller, with a slight increase in the offset for moderately logged forests (Fig. 4B).

The maximum offset presented the greatest differences among the three classes of logging intensity. While the offsets in heavily and moderately logged forests were negative, offsets in unlogged forests were positive. The variation in macroclimate led to changes in offsets from 0.3 °C to 1.6 °C in unlogged forests and from −2.3 °C to −3.9 °C in heavily logged forests (Fig. 4C). These results thus demonstrate that the forest capacity to buffer macroclimate variability, particularly in extreme climatic events, can be substantially affected even in moderately logged forests.

The range in the daily microclimate temperature was also strongly affected by logging (Fig. 4D). While the daily temperature range in unlogged forests increased by approximately 3.5 °C (from ~3.0 °C to 6.5 °C), the daily temperature range of heavily disturbed forests increased by ~6 °C (from ~5.9 °C to 12 °C).

Canopy structural traits had a strong influence on the capacity of forest to offset extreme temperatures. The CR and upper canopy PAI between 30 and 35 m had the highest contributions to explain the microclimate offset temperatures and range. The CR explained approximately 40 % of the variability in maximum offset temperature and the upper canopy PAI between 30 m and 35 m explained another 40 % (Fig. 5). These values, however, were not independent (i.e., some of the variability could be concomitantly explained by both variables). Considering all random and fixed variables, the model explained 84 %, 91 % and 73 % of the variability for the minimum, mean and maximum offset temperatures respectively, and 82 % of the range temperature. The fixed effects in the model alone explained 32 %, 51 %, 47 %, and 52 % for minimum, mean, maximum offset and range temperatures, respectively.

These results demonstrate the key role of forest structural traits, particularly the proportional distribution of plant material along the vertical profile, in regulating microclimate temperatures during extreme events. While the minimum temperature showed that the offset was more strongly driven by macroclimate anomalies, and proportionally less by structural attributes, the reverse was true for maximum

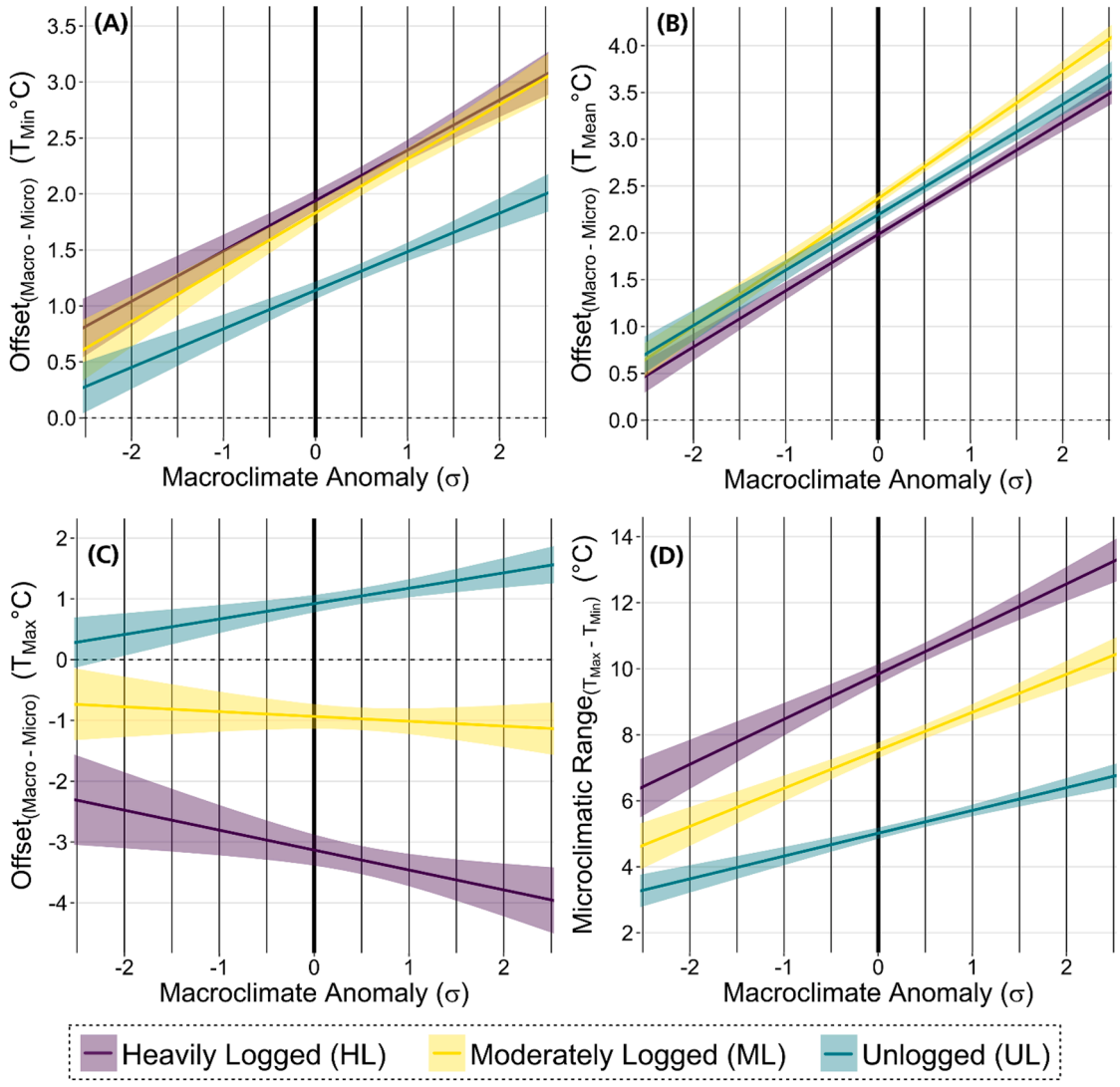


**Fig. 4.** The curves represent the modelled relationship based on mixed models of minimum (A), mean (B), maximum (C) offsets and range (D) for air temperature, where anomaly, CR and PAI(30–35) were fixed effects and plot id and the slope were random effects. The three colours represent heavily logged (purple), moderately logged (yellow), and unlogged (teal) forests.

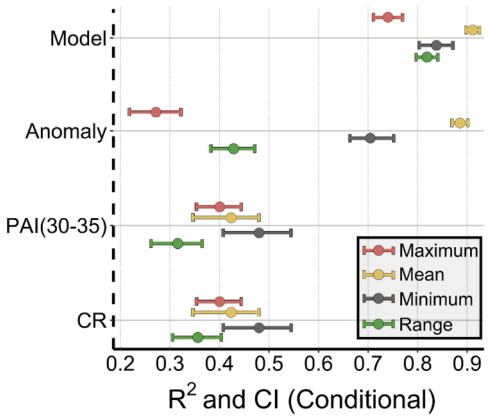


**Fig. 5.** Partitioning variance explained by the model and by each canopy trait included in the final model. The results show the conditional $R^2$ and confidence interval for each fixed variable in the model for minimum (grey), mean (yellow) maximum (red) offsets and range (green) after a 1000 bootstrap replication. See Table S.1 for a sensitivity analysis and S2 for the regression coefficient.

temperature offset (Fig. 5).

## 4. Discussion

High density terrestrial LiDAR combined with long-term microclimate measurements provided new insights into the contribution of physical forest attributes in regulating the thermal buffering capacity of tropical forests. We demonstrated that changes in structural traits, particularly those representing the vertical allocation of plant material, can substantially influence the capacity of forests to buffer large-scale temperature variability. We discuss the implications of these findings, their limitations, and how they can be inserted into a broader context to further expand our knowledge in this field.

### *4.1. Influence of forest structural traits on the microclimate*

Our results clarified how forest structural characteristics, as well as the changes in these characteristics caused by selective logging, affect the capacity of forests to offset macroclimatic variability. We found that traits representing the vertical distribution of vegetation within the forest are particularly useful to determine how well forests can offset macroclimate temperatures. In particular, the canopy ratio (CR) and the

material allocated in the highest layers between 30 m and 35 m (PAI 30–35) were successful in explaining a large part of the maximum offset variability, and these structural characteristics were strongly associated with forest disturbances (Santos et al., 2022; Maeda et al., 2022). In dense unlogged tropical forests, air temperature spikes can occur near the ground, but are more often experienced within the top canopy, where most of the incoming energy is absorbed (Didham and Ewers, 2014). Below tree canopies, reduced radiation and air mixing combined with evapotranspiration often translate into lower temporal variation in air temperature and humidity compared to open environments (Arx et al., 2013; Davis et al., 2019; Geiger et al., 2009; Haesen et al., 2023, 2021). Therefore, the characteristics of the vegetation layer between the soil and the atmosphere play a major role in regulating the spatial and temporal characteristics of the conditions experienced inside the forest. However, as demonstrated here, these dynamics are gradually changed with different levels of forest disturbance.

The CR values are higher in forests with relatively more vegetation in the understory (Maeda et al., 2022). This is typical of forests disturbed by logging, where canopy gaps created by the removal of trees increase the penetration of incoming solar radiation, and favour the growth of understory vegetation and thus increase the CR. Moreover, the removal of tall emergent trees also results in the reduction of vegetation in the upper layers of the canopy. This has direct implications in reducing the PAI(30–35).

The patterns of temperature offset differed for daytime (maximum offset) and nighttime (minimum offset). While the magnitude of the minimum offset was mainly driven by macroclimate conditions, the maximum offset was strongly influenced by forest structural characteristics (i.e., CR and PAI 30–35) (Fig. 5). These findings suggest that unlogged forests will likely become increasingly important in offsetting temperature anomalies in the future, in particular for the maximum temperature along projected increase in the frequency of extreme warm events (Solomon et al., 2007).

### 4.2. Diurnal variability

The biophysical mechanisms defining diurnal forest microclimate patterns are relatively well understood. During daytime, incoming solar radiation interacts with the forest canopy, and can either be reflected, transmitted or absorbed (Panferov et al., 2001). Of the fraction that is absorbed, some is used in photosynthesis, and some is transformed into heat in the leaves and forest layers. Selective logging leads to an abrupt reduction in the plant material allocated in the upper layers of the canopy, allowing more radiation to reach the ground and thus increasing the temperature near the forest surface. Forests with a more even vertical distribution of plant material, or a larger allocation in the upper layers, as in the case of plots in VJR (i.e., without recent selective logging), have more incoming radiation intercepted and higher roughness length, reducing wind speed and decreasing vertical mixing of air below the canopy (Raupach et al., 1996), consequently the temperature near the surface tends to be lower.

In unlogged forests, the canopy interaction with incoming shortwave solar radiation, combined with evaporative cooling, leads to a reduction of the understory daytime temperature on average 4.6 °C compared to open-field conditions. In contrast, nighttime temperatures of forest understories are on average 1 °C warmer, mainly as a result of canopy heat retention through shielding of the outgoing long-wave radiation by the canopy (De Frenne et al., 2019; Geiger et al., 2009). Our results reinforce the fact that, when evaluating only daily average values, these complex diurnal dynamics are lost, hiding important information for understanding the impacts of disturbances on the microclimate, as well as its response to macroclimate variability.

The overall diurnal temperature patterns reported in our results are in line with other studies that relate logging to microclimate temperature (Blonder et al., 2018; Hardwick et al., 2015; Jucker et al., 2018), whereby selectively logged forests presented higher microclimate temperature fluctuations. Often, the highest temperatures are recorded around midday. Since disturbed forests have less canopy material to intercept solar radiation and wind, they heat up more quickly than non-degraded forests. These characteristics reduce the buffer potential of the forest, which disrupts thermal inertia and leads to faster warming of the forest microclimate. (Zellweger et al., 2019).

However, some studies have indicated that selective logging has minimal impact on microclimate temperature (Senior et al., 2017a, 2017b). Nevertheless, in contrast to our study and those conducted in the SAFE area (Blonder et al., 2018; Hardwick et al., 2015; Jucker et al., 2018), Senior et al. (2017a) examined a continuous forest where the logged region was connected to an unlogged area. It is important to note that the logged forests defined by Senior et al. (2017a), are similar to what we considered as moderately logged (block LFE). Additionally, a crucial disparity between the studies lies in the spatial scale analysed. Senior et al. (2017a) defined macroclimate as the temperature recorded by dataloggers suspended within the forest, while we utilized temperature data from ERA5-Land at a scale of ~9 km as our macroclimate reference. Furthermore, in our study, microclimate measurements were taken at a height of 15 cm from the ground, whereas Senior et al. (2017a) regarded microclimate as the climate inside microhabitats, including tree holes, deadwood, and leaf litter. Another noteworthy distinction is the temporal scale examined. We conducted a comprehensive survey throughout the entirety of 2019, whereas Senior et al. (2017a) focused on a four-month period (April to July 2015). Considering these factors, the impact of forest degradation on microclimate temperature is contingent upon forest structure, the thermal metrics analysed, and primarily, the spatial-temporal scale considered.

### 4.3. Microclimatic seasonality along a selective logging gradient

Structural changes arising from selective logging alter albedo, reduce roughness and promote more sensible heat exchange over latent heat exchange. As demonstrated here, these disturbances result in a range of microclimatic temperature changes. However, the magnitude of these changes is also strongly dependent on geographical and temporal factors, such as latitude (Lee et al., 2011), altitude (Aalto et al., 2022), and local climate seasonality.

Throughout 2019, areas affected by selective logging showed minimum temperatures and daily averages cooler than the macroclimate temperatures. On the other hand, daily maximum temperatures were warmer than the macroclimate for all heavily logged forests. Given the relatively coarse resolution of the ERA5-Land dataset, the macroclimate temperatures for our plots were similar or equal to each other. This aligns with our initial assumption that the macroclimate represents the overall open-air temperature. The validity of this assumption is reinforced by the fact that the SAFE experiment was designed to minimize confounding factors associated with topographic and altitudinal differences (Ewers et al., 2011). Consequently, the different microclimate seasonal patterns observed in our plots are largely driven by the structural differences arising from the varied logging activities. The most noticeable impact was a greater microclimatic temporal variability in heavily logged forests, which has also been reported in previous studies (Blonder et al., 2018).

A larger seasonal variability in selectively logged forests indicates a lower capacity of the forest to buffer microclimate temperatures (De Frenne et al., 2013; Hardwick et al., 2015). Our results provide further evidence that disturbed forests may be more exposed to seasonal variability. While unlogged forests managed to buffer macroclimate seasonal fluctuations, logged forests experienced considerably more fluctuations throughout the year, including a higher temperature.

## 5. Conclusion

Our study quantified how structural changes arising from selective logging affect the capacity of tropical forests to offset large-scale climate

variability. We demonstrate that, to effectively identify how structural changes affect the microclimate, temperature patterns need to be analysed through different temporal scales, and with a careful consideration of both local and large-scale conditions. Forests affected by logging tended to be relatively shorter and with less vegetation allocated in the higher layers (i.e., 30 to 35 m). Consequently, disturbed forests presented a more uneven vertical distribution of plant material, with a higher concentration of vegetation in the understory. These changes affected energy partition and heat exchange within the canopy, reducing the potential of the forest to buffer temperatures below the canopy. When compared to unlogged forests, heavily logged forests tended to be warmer during the day and colder during the night. Logged forests presented larger seasonal fluctuations in the daytime temperature when compared to unlogged forests, thus showing a reduced capacity to alleviate intra-annual macroclimate variability. More importantly, we identified a strong decline in the capacity of logged forests to buffer extreme warm events, with differences between maximum temperatures inside and outside forests substantially increasing during anomalous warm days.

## CRediT authorship contribution statement

**Erone Ghizoni Santos:** Writing – review & editing, Writing – original draft, Visualization, Methodology, Formal analysis, Conceptualization. **Martin Svátek:** Writing – original draft, Resources, Data curation. **Matheus Henrique Nunes:** Writing – original draft, Methodology, Formal analysis, Data curation. **Juha Aalto:** Writing – original draft. **Rebecca A. Senior:** Writing – original draft. **Radim Matula:** Writing – original draft, Data curation. **Roman Plichta:** Writing – original draft, Data curation. **Eduardo Eiji Maeda:** Writing – review & editing, Writing – original draft, Supervision, Methodology, Funding acquisition, Formal analysis, Data curation, Conceptualization.

## Declaration of competing interest

The authors declare that they have no known competing financial interests or personal relationships that could have appeared to influence the work reported in this paper.

Eduardo Eiji Maeda reports financial support was provided by Academy of Finland. Martin Svátek reports financial support was provided by Ministry of Education, Youth and Sports of the Czech Republic.

## Data availability

Data will be made available on request.

## Acknowledgments

This study was funded by the Academy of Finland (decision numbers 318252, 319905, 345472, and 337552) and the Ministry of Education, Youth and Sports of the Czech Republic (grant nr. INTER-TRANSFER LTT19018). In addition, we would like to thank Dr. Noreen Majalap for her contribution and collaboration during TLS data collection, and Julsun (Joseph Bin Sikui) for his support. Also, we want to extend our thanks to the Sime Darby Foundation, the Sabah Foundation, Benta Wawasan and the Sabah Forestry Department for their support of the SAFE Project and Robert Ewers for heading the SAFE project. We thank the South East Asia Rainforest Research Partnership for logistical support in the field, and Yayasan Sabah, Maliau Basin Management Committee, the State Secretary, Sabah Chief Minister's Departments, the Malaysian Economic Planning Unit and the Sabah Biodiversity Centre for permission to conduct research in Sabah under the Access Licences number JKM/MBS.1000-2/2 JLD.9(111), and JPHTN/PSH 100-14/18/2/JLD.2(37). Lastly, we thank all people involved in the installation of the microclimate sensors and data collection.

## Supplementary materials

Supplementary material associated with this article can be found, in the online version, at doi:10.1016/j.agrformet.2024.109912.

## References

Aalto, I.J., Maeda, E.E., Heiskanen, J., Aalto, E.K., 2022. Strong influence of trees outside forest in regulating microclimate of intensively modified Afromontane landscapes. Biogeosciences 19, 4227–4247. https://doi.org/10.5194/bg-19-4227-2022.

Arx, G.Von, Pannatier, E.G., Thimonier, A., Rebetez, M., 2013. Microclimate in forests with varying leaf area index and soil moisture: potential implications for seedling establishment in a changing climate. J. Ecol. 101, 1201–1213. https://doi.org/10.1111/1365-2745.12121.

Bates, D., Mächler, M., Bolker, B., Walker, S., 2015. Fitting linear mixed-effects models using lme4. J. Stat. Softw. 67, 48. https://doi.org/10.18637/jss.v067.i01.

Béland, M., Widlowski, J.L., Fournier, R.A., Côté, J.F., Verstraete, M.M., 2011. Estimating leaf area distribution in savanna trees from terrestrial LiDAR measurements. Agric. For. Meteorol. 151, 1252–1266. https://doi.org/10.1016/j.agrformet.2011.05.004.

Blonder, B., Both, S., Coomes, D.A., Elias, D., Jucker, T., Kvasnica, J., Majalap, N., Malhi, Y.S., Milodowski, D., Riutta, T., Svátek, M., 2018. Extreme and highly heterogeneous microclimates in selectively logged tropical forests. Front. For. Glob. Chang. 1, 1–14. https://doi.org/10.3389/ffgc.2018.00005.

Bryan, J.E., Shearman, P.L., Asner, G.P., Knapp, D.E., Aoro, G., Lokes, B., 2013. Extreme differences in forest degradation in borneo: comparing practices in Sarawak, Sabah, and Brunei. PLoS One 8, 1–7. https://doi.org/10.1371/journal.pone.0069679.

Calders, K., Adams, J., Armston, J., Bartholomeus, H., Bauwens, S., Bentley, L.P., Chave, J., Danson, F.M., Demol, M., Disney, M., Gaulton, R., Krishna Moorthy, S.M., Levick, S.R., Saarinen, N., Schaaf, C., Stovall, A., Terryn, L., Wilkes, P., Verbeeck, H., 2020. Terrestrial laser scanning in forest ecology: expanding the horizon. Remote Sens. Environ. 251, 112102 https://doi.org/10.1016/j.rse.2020.112102.

Chen, J., Saunders, S.C., Crow, T.R., Naiman, R.J., Brosofske, K.D., Mroz, G.D., Brookshire, B.L., Franklin, J.F., 1999. Microclimate in Forest Ecosystem and Landscape Ecology: variations in local climate can be used to monitor and compare the effects of different management regimes. Bioscience 49, 288–297.

Davis, K.T., Dobrowski, S.Z., Holden, Z.A., Higuera, P.E., Abatzoglou, J.T., 2019. Microclimatic buffering in forests of the future: the role of local water balance. Ecography (Cop.) 42, 1–11. https://doi.org/10.1111/ecog.03836.

De Frenne, P., Lenoir, J., Luoto, M., Scheffers, B.R., Zellweger, F., Aalto, J., Ashcroft, M. B., Christiansen, D.M., Decocq, G., Pauw, K.De, Govaert, S., Greiser, C., Gril, E., Hampe, A., Jucker, T., Klinges, D.H., Koelemeijer, I.A., Lembrechts, J.J., Marrec, R., Meeussen, C., Ogée, J., Tyystjärvi, V., Vangansbeke, P., Hylander, K., Frenne, P.De, 2021. Forest microclimates and climate change: importance, drivers and future research agenda. Glob. Chang. Biol. 1–19. https://doi.org/10.1111/gcb.15569.

De Frenne, P., Rodríguez-Sánchez, F., Coomes, D.A., Baeten, L., Verstraeten, G., Vellen, M., Bernhardt-Römermann, M., Brown, C.D., Brunet, J., Cornelis, J., Decocq, G.M., Dierschke, H., Eriksson, O., Gilliam, F.S., Hédl, R., Heinken, T., Hermy, M., Hommel, P., Jenkins, M.A., Kelly, D.L., Kirby, K.J., Mitchell, F.J.G., Naaf, T., Newman, M., Peterken, G., Petřík, P., Schultz, J., Sonnier, G., Van Calster, H., Waller, D.M., Walther, G.R., White, P.S., Woods, K.D., Wulf, M., Graae, B. J., Verheyen, K., 2013. Microclimate moderates plant responses to macroclimate warming. Proc. Natl. Acad. Sci. U. S. A. 110, 18561–18565. https://doi.org/10.1073/pnas.1311190110.

De Frenne, P., Zellweger, F., Rodríguez-Sánchez, F., Scheffers, B.R., Hylander, K., Luoto, M., Vellend, M., Verheyen, K., Lenoir, J., 2019. Global buffering of temperatures under forest canopies. Nature Ecology & Evolution 3, 744–749. https://doi.org/10.1038/s41559-019-0842-1.

Didham, R.K., Ewers, R.M., 2014. Edge effects Disrupt vertical stratification of microclimate in a temperate forest canopy. Pacific Science 68, 493–508. https://doi.org/10.2984/68.4.4.

Drake, J.B., Dubayah, R.O., Knox, R.G., Clark, D.B., Blair, J.B., Rica, C., 2002. Sensitivity of large-footprint lidar to canopy structure and biomass in a neotropical rainforest. Remote Sens. Environ. 81, 378–392. https://doi.org/10.1016/S0034-4257(02)00013-5.

Ehbrecht, M., Schall, P., Juchheim, J., Ammer, C., Seidel, D., 2016. Effective number of layers: a new measure for quantifying three-dimensional stand structure based on sampling with terrestrial LiDAR. For. Ecol. Manage. 380, 212–223. https://doi.org/10.1016/j.foreco.2016.09.003.

Ellis, E.C., Gauthier, N., Goldewijk, K.K., Bird, R.B., Boivin, N., Díaz, S., Fuller, D.Q., Gill, J.L., Kaplan, J.O., Kingston, N., Locke, H., McMichael, C.N.H., Ranco, D., Rick, T.C., Rebecca Shaw, M., Stephens, L., Svenning, J.C., Watson, J.E.M., 2021. People have shaped most of terrestrial nature for at least 12,000 years. Proc. Natl. Acad. Sci. U. S. A. 118, 1–8. https://doi.org/10.1073/pnas.2023483118.

Ewers, R.M., Didham, R.K., Fahrig, L., Ferraz, G., Hector, A., Holt, R.D., Kapos, V., Reynolds, G., Sinun, W., Snaddon, J.L., Turner, E.C., 2011. A large-scale forest fragmentation experiment: the stability of altered forest ecosystems project. Philos. Trans. R. Soc. B Biol. Sci. 366, 3292–3302. https://doi.org/10.1098/rstb.2011.0049.

FAO, 2011. Assessing forest degradation: towards the development of globally applicable guidlines. For. Resour. Assess. 99. https://doi.org/10.1023/B:VEGE.0000029381.63336.20.

Fauset, S., Gloor, M.U., Aidar, M.P.M., Freitas, H.C., Fyllas, N.M., Marabesi, M.A., Rochelle, A.L.C., Shenkin, A., Vieira, S.A., Joly, C.A., 2017. Tropical forest light

regimes in a human-modified landscape. Ecosphere 8. https://doi.org/10.1002/ecs2.2002.
Fisher, B., Edwards, D.P., Giam, X., Wilcove, D.S., 2011. The high costs of conserving Southeast Asia's lowland rainforests. Front. Ecol. Environ. 9, 329–334. https://doi.org/10.1890/100079.
Fukami, T., Wardle, D.A., 2005. Long-term ecological dynamics: reciprocal insights from natural and anthropogenic gradients. Proc. R. Soc. B Biol. Sci. 272, 2105–2115. https://doi.org/10.1098/rspb.2005.3277.
Geiger, R., Aron, R.H., Todhunter, P., 2009. The Climate Near the Ground. Rowman & Littlefield.
Good, S.P., Noone, D., Bowen, G., 2015. Hydrologic connectivity constrains partitioning of global terrestrial water fluxes. Science 349 (80–), 175–178. https://doi.org/10.1126/science.aaa5931.
Gril, E., Spicher, F., Greiser, C., Ashcroft, M.B., Pincebourde, S., Durrieu, S., Nicolas, M., Richard, B., Decocq, G., Marrec, R., Lenoir, J., 2022. Slope and equilibrium : a parsimonious and flexible approach to model microclimate. Method. Ecol. Evol. 2023, 885–897. https://doi.org/10.1111/2041-210X.14048.
Haesen, S., Lembrechts, J.J., Frenne, P.De, Lenoir, J., Aalto, J., Ashcroft, M.B., Kopecký, M., Luoto, M., Kreyling, J., Kruijt, B., Macek, M., Máliš, F., Estrada, M.P., Schmeddes, J., Shekhar, A., Spicher, F., Ujházyová, M., Vangansbeke, P., Weigel, R., Wild, J., Zellweger, F., Meerbeek, K.Van, 2023. ForestClim — - Bioclimatic variables for microclimate temperatures of European forests. Glob. Chang. Biol. 2886–2892. https://doi.org/10.1111/gcb.16678.
Haesen, S., Lembrechts, J.J., Frenne, P.De, Lenoir, J., Aalto, J., Ashcroft, M.B., Kopecký, M., Luoto, M., Kreyling, J., Kruijt, B., Macek, M., Máliš, F., Estrada, M.P., Schmeddes, J., Shekhar, A., Spicher, F., Ujházyová, M., Vangansbeke, P., Weigel, R., Wild, J., Zellweger, F., Meerbeek, K.Van, 2021. ForestTemp – - Sub-canopy microclimate temperatures of European forests. Glob. Chang. Biol. 6307–6319. https://doi.org/10.1111/gcb.15892.
Hardwick, S.R., Toumi, R., Pfeifer, M., Turner, E.C., Nilus, R., Ewers, R.M., 2015. The relationship between leaf area index and microclimate in tropical forest and oil palm plantation: forest disturbance drives changes in microclimate. Agric. For. Meteorol. 201, 187–195. https://doi.org/10.1016/j.agrformet.2014.11.010.
Hersbach, H., Bell, B., Berrisford, P., Hirahara, S., Horányi, A., Muñoz-Sabater, J., Nicolas, J., Peubey, C., Radu, R., Schepers, D., Simmons, A., Soci, C., Abdalla, S., Abellan, X., Balsamo, G., Bechtold, P., Biavati, G., Bidlot, J., Bonavita, M., De Chiara, G., Dahlgren, P., Dee, D., Diamantakis, M., Dragani, R., Flemming, J., Forbes, R., Fuentes, M., Geer, A., Haimberger, L., Healy, S., Hogan, R.J., Hólm, E., Janisková, M., Keeley, S., Laloyaux, P., Lopez, P., Lupu, C., Radnoti, G., de Rosnay, P., Rozum, I., Vamborg, F., Villaume, S., Thépaut, J.N., 2020. The ERA5 global reanalysis. Q. J. R. Meteorol. Soc. 146, 1999–2049. https://doi.org/10.1002/qj.3803.
Hosonuma, N., Herold, M., De Sy, V., De Fries, R.S., Brockhaus, M., Verchot, L., Angelsen, A., Romijn, E., 2012. An assessment of deforestation and forest degradation drivers in developing countries. Environ. Res. Lett. 7 https://doi.org/10.1088/1748-9326/7/4/044009.
Isenburg, M., 2016. LASTools "Efficient LiDAR Processing Software".
Jucker, T., Hardwick, S.R., Both, S., Elias, D.M.O., Ewers, R.M., Milodowski, D.T., Swinfield, T., Coomes, D.A., 2018. Canopy structure and topography jointly constrain the microclimate of human-modified tropical landscapes. Glob. Chang. Biol. 24, 5243–5258. https://doi.org/10.1111/gcb.14415.
Katayama, A., Kume, T., Komatsu, H., Ohashi, M., Nakagawa, M., Yamashita, M., Otsuki, K., Suzuki, M., Kumagai, T., 2009. Effect of forest structure on the spatial variation in soil respiration in a Bornean tropical rainforest. Agric. For. Meteorol. 149, 1666–1673. https://doi.org/10.1016/j.agrformet.2009.05.007.
Kumar, R., Shahabuddin, G., 2005. Effects of biomass extraction on vegetation structure, diversity and composition of forests in Sariska Tiger Reserve, India. Environ. Conserv. 32, 248–259. https://doi.org/10.1017/S0376892905002316.
Lee, X., Goulden, M.L., Hollinger, D.Y., Barr, A., Black, T.A., Bohrer, G., Bracho, R., Drake, B., Goldstein, A., Gu, L., Katul, G., Kolb, T., Law, B.E., Margolis, H., Meyers, T., Monson, R., Munger, W., Oren, R., Paw U, K.T., Richardson, A.D., Schmid, H.P., Staebler, R., Wofsy, S., Zhao, L., 2011. Observed increase in local cooling effect of deforestation at higher latitudes. Nature 479, 384–387. https://doi.org/10.1038/nature10588.
MacArthur, R.H., MacArthur, J.W., 1961. On bird species diversity. Ecology 42, 594–598. https://doi.org/10.2307/1932254.
Maclean, I.M.D., Duffy, J.P., Haesen, S., Govaert, S., Frenne, P.De, Vanneste, T., Lenoir, J., Lembrechts, J.J., Rhodes, M.W., Meerbeek, K.Van, 2021. On the measurement of microclimate. Method. Ecol. Evol. 1397–1410. https://doi.org/10.1111/2041-210X.13627, 2021.
Maeda, E.E., Nunes, M.H., Calders, K., de Moura, Y.M., Raumonen, P., Tuomisto, H., Verley, P., Vincent, G., Zuquim, G., Camargo, J.L., 2022. Shifts in structural diversity of Amazonian forest edges detected using terrestrial laser scanning. Remote Sens. Environ. 271 https://doi.org/10.1016/j.rse.2022.112895.
Milodowski, D.T., Coomes, D.A., Swinfield, T., Jucker, T., Riutta, T., Malhi, Y., Svátek, M., Kvasnica, J., Burslem, D.F.R.P., Ewers, R.M., Teh, Y.A., Williams, M., 2021. The impact of logging on vertical canopy structure across a gradient of tropical forest degradation intensity in Borneo. J. Appl. Ecol. 58, 1764–1775. https://doi.org/10.1111/1365-2664.13895.
Muñoz Sabater, J., 2019. ERA5-Land Hourly Data from 1981 to Present. Copernicus Climate Change Service (C3S) Climate Data Store (CDS) [WWW Document]. https://doi.org/10.24381/cds.e2161bac.
Nakicenovic, N., Alcamo, J., Davis, G., De Vries, B., Fenhann, J., Gaffin, S., Gregory, K., Grubler, A., Jung, T.Y., Kram, T., 2000. A Special Report of Working Group III of the Intergovernmental Panel On Climate Change. Cambridge University Press, Cambridge.
NOAA, N.O. and A.A., 2019a. Nino Regions. URL. https://www.cpc.ncep.noaa.gov/products/analysis_monitoring/ensostuff/nino_regions.shtml.
NOAA, N.O. and A.A., 2019b. Cold and Warm Episodes by Season. URL. https://origin.cpc.ncep.noaa.gov/products/analysis_monitoring/ensostuff/ONI_v5.php.
Nunes, M.H., Jucker, T., Riutta, T., Svátek, M., Kvasnica, J., Rejžek, M., Matula, R., Majalap, N., Ewers, R.M., Swinfield, T., Valbuena, R., Vaughn, N.R., Asner, G.P., Coomes, D.A., 2021. Recovery of logged forest fragments in a human-modified tropical landscape during the 2015-16 El Niño. Nat. Commun. 12, 1–11. https://doi.org/10.1038/s41467-020-20811-y.
Panferov, O., Knyazikhin, Y., Myneni, R.B., Szarzynski, J., Engwald, S., Schnitzler, K.G., Gravenhorst, G., 2001. The role of canopy structure in the spectral variation of transmission and absorption of solar radiation in vegetation canopies. IEEE Trans. Geosci. Remote Sens. 39, 241–253. https://doi.org/10.1109/36.905232.
Pearson, T.R.H., Brown, S., Murray, L., Sidman, G., 2017. Greenhouse gas emissions from tropical forest degradation: an underestimated source. Carbon Balance Manag. 12 https://doi.org/10.1186/s13021-017-0072-2.
Pfeifer, M., Kor, L., Nilus, R., Turner, E., Cusack, J., Lysenko, I., Khoo, M., Chey, V.K., Chung, A.C., Ewers, R.M., 2016. Mapping the structure of Borneo's tropical forests across a degradation gradient. Remote Sens. Environ. 176, 84–97. https://doi.org/10.1016/j.rse.2016.01.014.
Pfeifer, M., Lefebvre, V., Turner, E., Cusack, J., Khoo, M.S., Chey, V.K., Peni, M., Ewers, R.M., 2015. Deadwood biomass: an underestimated carbon stock in degraded tropical forests? Environ. Res. Lett. 10 https://doi.org/10.1088/1748-9326/10/4/044019.
Pickett, S.T.A., 1989. Space-for-time substitution as an alternative to long-term studies. Long-Term Stud. Ecol 110–135. https://doi.org/10.1007/978-1-4615-7358-6_5.
Pickett, S.T.A., White, P.S., 1985. No The Ecology of Natural Disturbance and Patch Dynamics.
R Core Team, 2020. R: A Language and Environment for Statistical Computing.
Raupach, M.R., Finnigan, J.J., Brunet, Y., 1996. Coherent eddies and turbulence in vegetation canopies: the mixing-layer analogy. Bound.-Layer Meteorol. 78, 351–382. https://doi.org/10.1007/BF00120941.
Reynolds, G., Payne, J., Sinun, W., Mosigil, G., Walsh, R.P.D., 2011. Changes in forest land use and management in Sabah, Malaysian Borneo, 1990-2010, with a focus on the Danum Valley region. Philos. Trans. R. Soc. B Biol. Sci. 366, 3168–3176. https://doi.org/10.1098/rstb.2011.0154.
Riutta, T., Malhi, Y., Kho, L.K., Marthews, T.R., Huaraca Huasco, W., Khoo, M.S., Tan, S., Turner, E., Reynolds, G., Both, S., Burslem, D.F.R.P., Teh, Y.A., Vairappan, C.S., Majalap, N., Ewers, R.M., 2018. Logging disturbance shifts net primary productivity and its allocation in Bornean tropical forests. Glob. Chang. Biol. 24, 2913–2928. https://doi.org/10.1111/gcb.14068.
Santos, E.G., Nunes, M.H., Jackson, T., Maeda, E.E., 2022. Quantifying tropical forest disturbances using canopy structural traits derived from terrestrial laser scanning. For. Ecol. Manage. 524, 120546 https://doi.org/10.2139/ssrn.4145312.
Schneider, F.D., Ferraz, A., Hancock, S., Duncanson, L.I., Dubayah, R.O., Pavlick, R.P., Schimel, D.S., 2020. Towards mapping the diversity of canopy structure from space with GEDI. Environ. Res. Lett. 15, 115006 https://doi.org/10.1088/1748-9326/ab9e99.
Schneider, F.D., Kükenbrink, D., Schaepman, M.E., Schimel, D.S., Morsdorf, F., 2019. Quantifying 3D structure and occlusion in dense tropical and temperate forests using close-range LiDAR. Agric. For. Meteorol. 268, 249–257. https://doi.org/10.1016/j.agrformet.2019.01.033.
Schneider, F.D., Leiterer, R., Morsdorf, F., Gastellu-Etchegorry, J.P., Lauret, N., Pfeifer, N., Schaepman, M.E., 2014. Simulating imaging spectrometer data: 3D forest modeling based on LiDAR and in situ data. Remote Sens. Environ. 152, 235–250. https://doi.org/10.1016/j.rse.2014.06.015.
Schneider, F.D., Morsdorf, F., Schmid, B., Petchey, O.L., Hueni, A., Schimel, D.S., Schaepman, M.E., 2017. Mapping functional diversity from remotely sensed morphological and physiological forest traits. Nat. Commun. 8 https://doi.org/10.1038/s41467-017-01530-3.
Senior, R.A., Hill, J.K., Benedick, S., Edwards, D.P., 2017a. Tropical forests are thermally buffered despite intensive selective logging. Glob. Chang. Biol. 24, 1267–1278. https://doi.org/10.1111/gcb.13914.
Senior, R.A., Hill, J.K., del Pliego, P.G., Goode, L.K., Edwards, D.P., 2017b. A pantropical analysis of the impacts of forest degradation and conversion on local temperature. Ecol. Evol. 7897–7908. https://doi.org/10.1002/ece3.3262.
Smith, D.L., Johnson, L., 2004. Vegetation-mediated changes in microclimate reduce soil respiration as woodlands expand into grasslands. Ecology 85, 3348–3361. https://doi.org/10.1890/03-0576.
Solomon, S., Qin, D., Manning, M., Chen, Z., Marquis, M., Averyt, K.B., Tignor, M., Miller, H.L., 2007. IPCC, 2007: climate change 2007: the physical science basis. Contribution of Working Group I to the Fourth Assessment Report of the Intergovernmental Panel On Climate Change. Cambridge Univ Press, Cambridge, UK.
Stevens, J.T., Safford, H.D., Harrison, S., Latimer, A.M., 2015. Forest disturbance accelerates thermophilization of understory plant communities. J. Ecol. 103, 1253–1263. https://doi.org/10.1111/1365-2745.12426.
Stoffel, M.A., Nakagawa, S., Schielzeth, H., 2020. partR2 : partitioning R 2 in generalized linear mixed models. bioRxiv. https://doi.org/10.1101/2020.07.26.221168.
Struebig, M.J., Turner, A., Giles, E., Lasmana, F., Tollington, S., Bernard, H., Bell, D., 2013. Quantifying the biodiversity value of repeatedly logged rainforests. gradient and comparative approaches from Borneo. Adv. Ecol. Res. 48, 183–224. https://doi.org/10.1016/B978-0-12-417199-2.00003-3.
Vincent, G., Antin, C., Laurans, M., Heurtebize, J., Durrieu, S., Lavalley, C., Dauzat, J., 2017. Mapping plant area index of tropical evergreen forest by airborne laser

scanning. A cross-validation study using LAI2200 optical sensor. Remote Sens. Environ. 198, 254–266. https://doi.org/10.1016/j.rse.2017.05.034.

Walsh, R.P.D., Newbery, D.M., 1999. The ecoclimatology of Danum, Sabah, in the context of the world's rainforest regions, with particular reference to dry periods and their impact. Philos. Trans. R. Soc. B Biol. Sci. 354, 1869–1883. https://doi.org/10.1098/rstb.1999.0528.

Wild, J., Kopecký, M., Macek, M., Šanda, M., Jankovec, J., Haase, T., 2019. Climate at ecologically relevant scales: a new temperature and soil moisture logger for long-term microclimate measurement. Agric. For. Meteorol. 268, 40–47. https://doi.org/10.1016/j.agrformet.2018.12.018.

Wilkes, P., Lau, A., Disney, M., Calders, K., Burt, A., Gonzalez, J., Tanago, D., Bartholomeus, H., Brede, B., Herold, M., Gonzalez de Tanago, J., Bartholomeus, H., Brede, B., Herold, M., 2017. Data acquisition considerations for Terrestrial Laser Scanning of forest plots. Remote Sens. Environ. 196, 140–153. https://doi.org/10.1016/j.rse.2017.04.030.

Yilmaz, M., 2023. Accuracy assessment of temperature trends from ERA5 and ERA5-Land. Sci. Total Environ. 856, 159182 https://doi.org/10.1016/j.scitotenv.2022.159182.

Zellweger, F., Coomes, D., Frenne, P.De, Lenoir, J., Rocchini, D., 2019. Advances in microclimate ecology arising from remote sensing. Trend. Ecol. Evol. 34, 327–341. https://doi.org/10.1016/j.tree.2018.12.012.

Zhao, P., He, Z., Ma, D., Wang, W., 2023. Evaluation of ERA5-land reanalysis datasets for extreme temperatures in the qilian mountains of China. Front. Ecol. Evol. 11, 1–13. https://doi.org/10.3389/fevo.2023.1135895.

Zou, J., Lu, N., Jiang, H., Qin, J., Yao, L., Xin, Y., Su, F., 2022. Performance of air temperature from ERA5-Land reanalysis in coastal urban agglomeration of Southeast China. Sci. Total Environ. 828, 154459 https://doi.org/10.1016/j.scitotenv.2022.154459.